Deutsches Zentrum
für Luft- und Raumfahrt e.V.
in der Helmholtz-Gemeinschaft

# EnMAP Ground Segment

## Level 1B Processor (Systematic and Radiometric Correction) ATBD

*Restriction: Public*

| | |
|---|---|
| Doc. ID | EN-PCV-TN-4006 |
| Issue | 1.8 |
| Date | 03.04.2023 |

Under Configuration Control: Yes

German Remote Sensing Data Center (DFD)
Remote Sensing Technology Institute (IMF)
German Space Operation Center (GSOC)

– blank page –

# TABLE OF SIGNATURES

**Prepared**

Miguel Pato

Digitally signed by Miguel Pato
DN: C=DE, OU=IMF-PBA, O=DLR, CN=Miguel Pato, E=miguel.figueiredovazpato@dlr.de
Reason: I am the author of this document
Location: Munich
Date: 2023.04.03 17:05:47+02'00'
Foxit PDF Reader Version: 12.1.1

Date — Miguel Pato
Subsystem Engineer DEV

Martin Bachmann

Digital signiert von Martin Bachmann
DN: OU=DFD-LAX, O=Deutsches Zentrum fuer Luft- und Raumfahrt e.V. (DLR), CN=Martin Bachmann, E=martin.bachmann@dlr.de
Grund: Ich bin der Verfasser dieses Dokuments
Ort:
Datum: 2023.04.17 09:05:29+02'00'
Foxit PDF Reader Version: 12.1.1

Date — Martin Bachmann
Subsystem Manager CGC

**Reviewed**

David Marshall

Digital signiert von David Marshall
DN: C=DE, O=DLR, CN=David Marshall, E=david.marshall@dlr.de
Grund: Ich bin der Verfasser dieses Dokuments
Ort: Weßling
Datum: 2023.04.17 10:43:24+02'00'
Foxit PDF Reader Version: 12.1.1

Date — David Marshall
Subsystem Manager SRC

**Approved**

Miguel Pato

Digitally signed by Miguel Pato
DN: C=DE, OU=IMF-PBA, O=DLR, CN=Miguel Pato, E=miguel.figueiredovazpato@dlr.de
Reason: I am approving this document
Location: Munich
Date: 2023.04.17 11:07:31+02'00'
Foxit PDF Editor Version: 12.1.1

Date — Miguel Pato
System Manager PCV

**Released**

Emiliano Carmona

Digitally signed by Emiliano Carmona
DN: C=DE, CN=Emiliano Carmona, E=Emiliano.Carmona@dlr.de
Reason: I am releasing this document
Location:
Date: 2023.04.18 09:04:25+02'00'
Foxit PDF Reader Version: 12.1.1

Date — Emiliano Carmona
GS Project Manager

– blank page –

# DISTRIBUTION LIST

This EnMAP Ground Segment document is stored in the Design Definition File (DDF) of the EnMAP Ground Segment Teamsite.

This document is accessible by all participants of the EnMAP Ground Segment as well as by the EnMAP Ground Segment Customer. This document may be further distributed by the EnMAP Project Management as necessary.

After commissioning the phase, the document is provided to the EnMAP user community on www.enmap.org.

# CHANGE RECORD

| Version | Date | Chapter | Comment |
|---|---|---|---|
| 0.9 | 17.05.2010 | all | Version for internal use |
| 1.0 | 07.06.2010 | all | Version for CDR |
| 1.1 | 02.11.2010 | 3.1 | Chapter is added for definition and indexing of image cube |
| | | 4.2 | Answer to RID KAU-H-0221 included |
| | | 4.10 | Output variable is changed to $DN_{VNIR}$ in formulae (4.10-1) (RID LAN-R-0280) |
| | | 4.13 | 670 nm is taken for green band in VNIR QL (RID LAN-R-0281) |
| | | 4.2 | Common indices are introduced for image data |
| | | 4.14 | Definition of band index is explained more clearly (RID LAN-R-0282) |
| | | 4.14 | Wavelengths are added (RID VON-A-0309) |
| | 21.10.2010 | 4.15 | Data QC parameters separately for VNIR and SWIR cameras [LAN-R-0271] |
| | 21.10.2010 | 4.15 | Dead Pixel screening (instrument monitoring) included in data QC [LAN-R-0272] |
| 1.2 | 01.04.2011 | 4.14 | Chapter is revised (RID VON-A-0307) |
| | 16.05.2011 | 4.11 | Clarification is added to show a common understanding of S/S and G/S (STR-C-0241) |
| 1.3 | 07.03.2016 | all | Added Detector Map component and corresponding workflow [SCR-00033] |
| | 09.03.2016 | 4 | Changed structure. All L1B processor steps are now contained in section 4 |
| | 09.03.2016 | 4.3 | Updated all relevant formulas |
| | 09.03.2016 | 4.5 (number in version 1.2) | Removed all contributions of Erik Borg because AC2020 |
| | 28.04.2016 | 4.13, 4.14 (number in version 1.2) | QL generation and quality masks generation moved to L0 ATBD document (EN-PCV-TN-3006 Level 0 Processor (Transcription and Screening) ATBD |
| | 29.04.2016 | all | Added input-output tables (RID LAN-R-0274) |
| | 03.05.2016 | 4.3.6 | New stray light correction algorithm (RID LAN-R-0278 thus obsolete) |
| | 03.05.2016 | 4.3.2 | Pixel flagging based on the L0 product (RID LAN-R-0277) |
| 1.4 | 28.09.2017 | 4 | Updated Sections 4.1, 4.2, 4.3.3-4.3.10. (incl. ICR-00085-1, SCR-00085) |
| | 30.05.2018 | 4 | Re-organised and updated Chapter 4 to reflect changes to L1B processor due to SCR-00111 (Implementation of defective pixel interpolation and smile correction). Update of outdated descriptions of L1B processing steps. |
| | 05.06.2018 | all | Updated Sec. 1.2. Updated format with compatibility mode to be able to edit figures and equations. |
| | 13.06.2018 | 4.3.5 | Updated dark signal filtering and interpolation. |
| | 18.06.2018 | 4.4.1 | Extended Raw Detector Maps (now separate for low & high gain), in accordance with L0 product definition EN-PCV-ICD-2009-1. NOTE: as the Detector Maps are a TAR.GZ component in the product model and thus no change in the interfacing to DIMS, there are no further changes in the product model or interfacing required. |
| | 04.10.2018 | 4.3 | Added block diagram for L1B_rad processor. |
| | 19.10.2018 | | Updated version of issue in preparation for release before GS-TVVRR. |
| | 12.11.2018 | 4 | Improved Figs. 4-1, moved quality from L0 ATDB, updated TBC/TBD list, cleaned old comments, updated issue version. |
| | 13.11.2018 | 4.1 | Updated Fig. 4-1. |
| | 15.11.2018 | 4.3, 4.7 | Added TBC-2 regarding SWIR gain switch row. |
| | 23.11.2018 | | Updated format and contents. |
| | 26.11.2018 | 2 | Updated issues of references, corrected typos. |
| | 28.11.2018 | all | Updated format, corrected typos. |
| | 29.11.2018 | all | Finalised document for release of issue 1.4. |
| 1.5 | 06.09.2019 | 4.3, 5 | Major modifications due to L1B implementation changes: VNIR gain bit (open issue PROC-7, L0/L1B task #22); SWIR gain mask from L0 metadata (SCR-00181; open issue CAL-1; L0/L1B task #6); dark signal computation (open issue CAL-15; L0/L1B task #19). Updated TBC / TBD. |
| | 05.05.2020 | All<br>4.4.2.1 | General update of document and references<br>Update of Dead Pixel Mask workflow (SCR-00208) |
| | 23.10.2020 | | Added Kevin Alonso as reviewer; updated reference issues; small editorial changes; modifications due to non-linearity correction (SCR-00206; open issue CAL-2; L0/L1B task #9); updated TBC / TBDs. |
| | 26.10.2020 | | Added David Marshall as contributor |

| | | | |
|---|---|---|---|
| | | 4.4.5 | SCR 00111 Added smile indication test |
| | | 4.4.2.1 | SCR 00213, SCR 00208, small modification of updated handling of the DeadPixelMask |
| | 16.11.2020 | all | Editorial changes before internal review. |
| | 26.11.2020 | | Editorial changes following internal review. Preparing issue 1.5. |
| 1.6 | 24.02.2021 | 4.3.2 | Modifications due to changes in SWIR gain during dark frames in Earth datatakes (svn ticket #202, SCR-00230). |
| | 25.02.2021 | 4.3 | Modifications due to swapping of RNU and straylight correction steps (svn ticket #174, SCR-00227). Former TBD-4 deleted. |
| | 14.09.2021 | 4.3.8 | Added description of straylight correction algorithm (trac ticket #132, SCR-00271). Former TBD-3 (straylight correction) deleted. |
| | 26.10.2021 | 4.4 | Minor updates (internal bit coding, QC-internal processing sequence), and added comment reg. “smile indication” as TBD-5 |
| | 02.11.2021 | 4.3.2 | Indicated that SWIR gain mask is taken from new CTB_RAD component instead of L0 metadata due to SWIR ROIC inconsistent behaviour (trac ticket #215, SCR-00272). |
| | 23.11.2021 | 4.4.6.2<br>4.4.8 | Updated blooming flagging for SWIR (ICR 230-07, SCR-00230)<br>Updated units in metadata from percent to permille, better reflecting the instrument properties after TVAC (ICR 230-07, SCR-00230) |
| | 30.11.2021 | 4.4.8 | Updated handling of QC parameter “status” (related to screening NCR-276) |
| | 10.12.2021 | 4.3.8 | Changed data type of straylight extraction matrices (trac tickets #234, #237, SCR-00271). |
| | 21.12.2021 | 2.1, 5 | Updated issues of applicable references. Deleted TBC-1 (Lunar datatakes, SCR-00113). |
| | 17.01.2022 | | Adapted TBD-1 (Dark pixels and bands). |
| | 18.01.2022 | | Removed TBD-1 (Dark pixels and bands), reorganized list of TBC / TBDs. Prepared issue 1.6. |
| 1.7 | 23.03.2022 | 4.4.5, 4.4.7., 4.4.8 | DSHA radiation issue (SCR-00302), added description of QC workflow for handling DSHA-affected data |
| | 19.07.2022 | 4.4.1, 4.4.2 | Updated the dimensions of the Detector Maps according to the latest number of bands of VNIR & SWIR in standard configuration (see Trac Ticket #300) |
| | 21.09.2022 | 4.4.7.2 | Update of saturation threshold (see Trac Ticket #248) |
| | 27.09.2022 | 4.4.x | Resolved TBDs for Commissioning Phase:<br>TBD-1 (thresholds for QC), TBD-2 (defects to be interpolated),<br>TBD-3 (spectral smile test), TBD-4 (DSHA defect interpolation) |
| | 04.10.2022 | 2.1, 4.5, 5 | Removed resolved TBDs. Updated ATBD and ICD issues in applicable references. Adapted comment regarding overlapping VNIR and SWIR bands in Sec. 4.5. Replaced Kevin Alonso by David Marshall as reviewer. Prepared issue 1.7 for public release. |
| 1.8 | 13.03.2023 | 4.1, 4.3.7, 4.3.9, 4.5 | Added description of destriping algorithm in Sec. 4.5 (FQR RID WER-RO-0004, SCR-00351) and adapted L1B processor overview in Sec. 4.1. Added description of VNIR dynamic coefficients in Secs. 4.3.7 and 4.3.9 (FQR RID WER-RO-0003, SCR-00322). Updated table of signatures (Miguel Pato as new System Manager PCV, Emiliano Carmona as new GS Project Manager) and added Maximilian Brell as contributor. |
| | 28.03.2023 | 4.5 | Adapted description of destriping algorithm based on feedback from Maximilian Brell (FQR RID WER-RO-0004, SCR-00351). |
| | 03.04.2023 | | Prepared issue 1.8 for public release. |

# DOCUMENT PREPARATION

The EnMAP *Level 1B Processor ATBD* Document was prepared with contributions from personnel as listed below.

| Name | Organizational Unit | Chapters |
|---|---|---|
| Martin Bachmann | DLR, DFD-LAX | 4.4 |
| David Marshall | DLR, DFD-LAX | 4.4 |
| Gintautas Palubinskas | DLR, MF-PBA | previous issues |
| Peter Gege | DLR, MF-EXV | previous issues |
| Thomas Walzel | DLR, MF-PBA | previous issues |
| Jakub Bieniarz | DLR, MF-PBA | previous issues |
| Miguel Pato | DLR, MF-PBA | all |
| Maximilian Brell | GFZ | 4.5 |

Custodian of this document is Pato, Miguel.

# CONTENTS

– blank page –

# LIST OF FIGURES



# LIST OF TABLES

– blank page –

# 1. Introduction

## 1.1 Purpose

This document explains the processing steps for EnMAP Level 1B product. In particular, the mathematical formulations and algorithmic approaches necessary for every step are outlined in detail.

## 1.2 Scope

This document describes the algorithms for data processing leading to the creation of EnMAP Level 1B product. Some of the chapters are based on algorithms presented in [AR-4] and thus only a short description will be given. The algorithms presented here are subject to modification as the camera delivery and characterisation proceeds.

# 2. References

## 2.1 Applicable references

The following documents are applicable to the extent specified herein.

| Document ID | Document Title | Issue |
|---|---|---|
| AR-1 | EN-KT-DD-001 EnMAP Design Document – Instrument, Volume III | 4.0 |
| AR-2 | EN-OHB-ICD-005 X-Band Data Definition | 7.0 |
| AR-3 | EN-KT-PL-005 Calibration & Characterisation Plan | 6.0 |
| AR-4 | EN-KT-TN-031 Algorithms for Data Processing | 9.0 |
| AR-5 | EN-KT-TN-060 Instrument Measurement Data Definition | 6.0 |
| AR-6 | EN-PCV-TN-8005 HSI Geometric Calibration and Quality Control Concept | 1.2 |
| AR-7 | EN-PCV-TN-1004 Definition of Product Levels | 1.2 |
| AR-8 | EN-PCV-ICD-2009-1 EnMAP HSI Level 0 Product Specification Document | 1.6 |
| AR-9 | EN-PCV-ICD-2009-2 EnMAP HSI Level 1 / Level 2 Product Specification Document | 1.8 |
| AR-10 | EN-PCV-TN-5006 Level 1C Processor (Geometric Correction) ATBD | 1.6 |
| AR-11 | EN-PCV-ICD-7008 Calibration Data Product Description | 1.7 |
| AR-12 | EN-PCV-ICD-2002 PCV-Internal-ICD | 1.5 |
| AR-13 | EN-PCV-RSP-2013 PCV System Requirements Specification | 1.3 |
| AR-14 | EN-PCV-DD-2004 Processor Design Document | 1.6 |
| AR-15 | EN-PCV-TN-6007 Level 2A Processor (Atmospheric Correction – Land) ATBD | 2.2 |
| AR-16 | EN-PGS-ICD-6013 Level-0 and Calibration Data Archive Products Specification | 1.4 |
| AR-17 | EN-GS-ICD-2032 Acquisition Station Data Product Specification | 1.6 |
| AR-18 | EN-PGS-ICD-6012 Orbit and Attitude Archive Products Specification | 1.2 |
| AR-19 | EN-PCV-TN-3006 Level 0 Processor Transcription and Screening ATBD | 1.7 |
| AR-20 | EN-PCV-TN-7010 Measurement and correction of stray light in imaging spectrometers | 1.0 |
| AR-21 | EN-PCV-DD-8004 QC Design Document | 1.1 |
| AR-22 | EN-GS-TN-1009 EnMAP Glossary and Abbreviations | 2.0 |
| AR-23 | EN-PCV-TN-6008 Level 2A Processor (Atmospheric Correction over Water) ATBD | 3.1 |
| AR-24 | EN-KT-TN-195 Inputs to GS for Science Data Processing | 4.0 |
| AR-25 | EN-IMF-TN-001 Stray Light Measurement & Correction of the EnMAP Instrument | 0.0 |
| AR-26 | EN-IMF-RP-004 EnMAP Calibration Support - Stray Light Calibration Report | 1.0 |

**Table 2-1 Applicable references.**

# 3. Terms, Definitions and Abbreviations

Terms, definitions and abbreviations for the EnMAP Ground Segment are collected together with those for the EnMAP Space Segment in a database which is publicly accessible via Internet on the EnMAP Information Portal [AR-22]:

http://www.enmap.org/

(menu item: Glossary & Abbr.)

## 3.1 Definition and indexing of image cube

Within this document the following understanding of terms will be used:

Let $i, j, k \in \mathrm{N}$ be the natural number indices representing coordinates in *3D* space (spatial-spatial-spectral), which are mapped to special physical meanings like digital number $DN_{i,j,k}$, radiance $L_{i,j,k}$ or reflectance $r_{i,j,k}$, with the following definitions

***i*** is the spatial coordinate defined by consecutive sensor exposures increasing with time ***t***, also called *along track* direction.

***j*** is the spatial coordinate defined by the timely read out sequence of a row or sensor line (physical numbering), also called across track direction. It is noted that the definition of the direction and origin can be changed depending on the definition of the coordinate frame.

***k*** is the spectral coordinate increasing from lower to higher wavelengths.

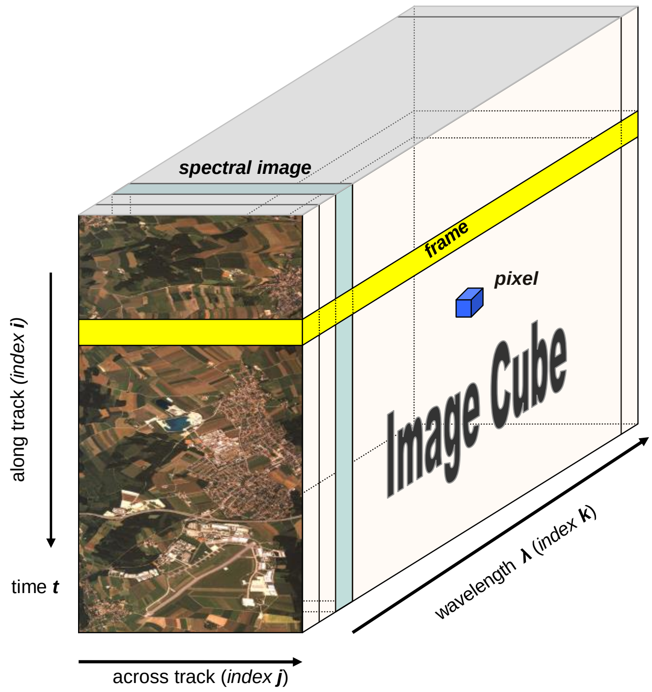


**Figure 3-1 EnMAP image data cube.**

The following spaces and sub-spaces are defined:

| Space | Definition | Identifier | Synonyms | Comment |
|---|---|---|---|---|
| 3-dimensional | all ***i,j,k*** are variable | image cube | • cube<br>• volumetric image<br>• image | |
| 2-dimensional | ***i*** is fixed ***j,k*** are variable | Frame | • read out<br>• frame read out | |

| | | | | |
|---|---|---|---|---|
| | ***k*** is fixed ***i,j*** are variable | spectral image | • channel<br>• spectral channel<br>• channel file<br>• band | A virtual channel contains additional information |
| | ***j*** is fixed ***i,k*** are variable | | | No practical usage |
| 1-dimensional | ***i*** is variable ***j,k*** are fixed | Column | | |
| | ***j*** is variable ***i,k*** are fixed | Row | • sensor line<br>• read out index ROI<br>• scan line | The ROI defines the actual transferred data |
| | ***k*** is variable ***i,j*** are fixed | spectral pixel vector | • spectrum<br>• pixel vector | |
| 0-dimensional | ***i,j,k*** are fixed | Pixel | • sample<br>• voxel | Smallest unit, which can be addressed. Often used as entity. |

# 4. L1B Processing

## 4.1 Overview

L1B is the first of the high-level processors and its central role is to transform the L0 raw data into a calibrated and spectrally referenced radiometric product. It is also at this level that comprehensive quality information is derived for both raw and calibrated image data. A complete list of L1B requirements can be found in [AR-13].

Because L1B shall optionally include smile correction, the other high-level processors need to be run in order to create the final L1B product, as illustrated in Figure 4-1. The focus of the current document is on the L1B_rad and destriping sub-processors; the other processors are described elsewhere: L1C in [AR-10], L1B_int and L2A in [AR-15, AR-23].

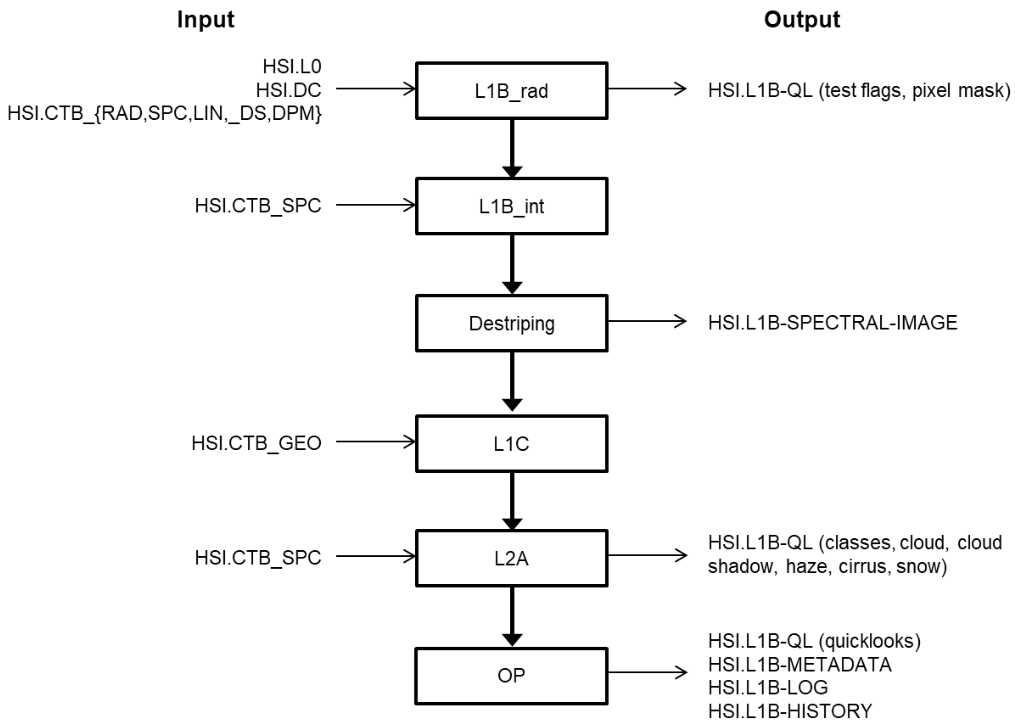


**Figure 4-1 Schematic pipeline of L1B processing. The naming of the inputs and outputs follows [AR-9, AR-18, AR-16]. A more detailed pipeline can be found in [AR-14].**

## 4.2 Input

The L1B processor requires the following input:

- **L0 product (HSI.L0)**, corresponding to one tile of an Earth datatake. This product contains the raw spectral images to be radiometrically calibrated along with the associated virtual channels. See [AR-8] for a full description of the L0 product.

- **DC product (HSI.DC)**, corresponding to the dark measurements taken during the datatake of the L0 product above. This product contains the raw spectral images of the dark phases before and after the imaging phase along with the associated virtual channels. See [AR-8] for a full description of the DC product.

- **Calibration tables (HSI.CTB_{RAD,SPC,LIN,_DS,DPM,GEO})**. The radiometric, spectral and geometric information needed to calibrate the raw images is stored in several calibration tables. The content and format of these tables are specified in [AR-11, AR-16].

The inputs for L1B processing are listed in Figure 4-1; for more detailed information, please refer to [AR-14].

## 4.3 L1B_rad

The L1B_rad sub-processor is designed to convert the raw values of an L0 tile into calibrated at-sensor radiances, applying in the process dark signal, non-linearity, gain matching and possibly straylight corrections. Only L0 tiles of Earth datatakes are supported for L1B processing. In order to fully characterise the final L1B product, L1B_rad also collects quality information before and after calibration. The outputs of this sub-processor include a calibrated radiance image cube and a 3D defective pixel mask. L1B_int shall use these as input to appropriately interpolate defective pixels.

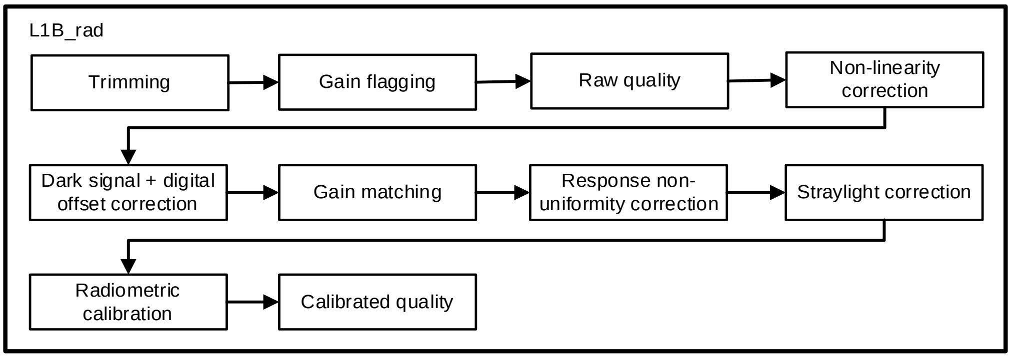


**Figure 4-2 Block diagram of L1B_rad processor.**

L1B_rad comprises the following steps described in detail in the coming sub-sections and illustrated in Figure 4-2:

1. Trimming
2. Gain flagging
3. Raw quality
4. Non-linearity correction
5. Dark signal and digital offset correction
6. Gain matching
7. Response non-uniformity correction
8. Straylight correction
9. Radiometric calibration

10. Calibrated quality

The data processing algorithms (see points 4 through 9 above) have been developed by the instrument experts at OHB and presented in [AR-4]. A self-contained description of the algorithms is outlined in the present document; full details and discussion can be found in the above mentioned reference.

All L1B_rad steps described in the following collect varied metadata information relevant for the L1B product. This information ends up in the L1B metadata file, which is thoroughly defined in [AR-9].

### 4.3.1 Trimming

As mentioned in [AR-19], not all transmitted spatial pixels and channels are illuminated. In fact, a variable number of spatial pixels (typically, 12 on each side) and of channels (typically, 2-6 in the top and bottom) are covered by the instrument and record essentially dark signal and eventually straylight. The non-illuminated rows (i.e., channels) and columns (i.e., pixels) are identified in the calibration table metadata (cf. [AR-11]) and the first step in L1B_rad is to trim these off the L0 and DC products, as illustrated in Figure 4-3. The resulting dimensions of L1B spectral images are typically:

- $N_{\mathrm{F}} \times 131 \times 1000$ for SWIR; and
- $N_{\mathrm{F}} \times 91 \times 1000$ for VNIR,

where the number of frames $N_{\mathrm{F}}$ is 1024 for L1B images derived from an L0 product and usually 256 for L1B images derived from each dark phase in the DC product. Notice that the number and configuration of the dark pixels and channels is may change during the mission. In the following, an L1B image cube shall be denoted by a 3D tensor $X$ in BIL format (frames x channels x pixels).

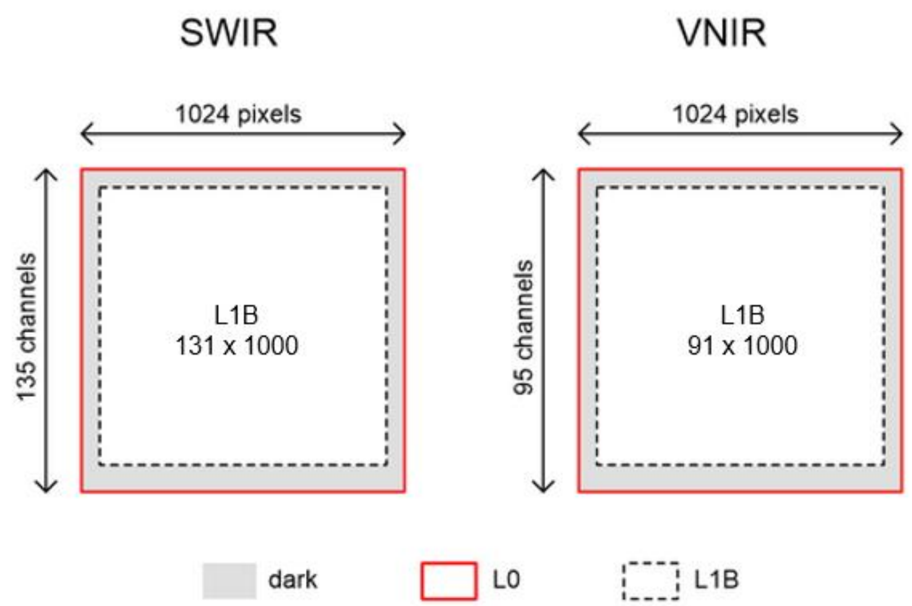


**Figure 4-3 Relative dimensions of the L0 product and the image cube processed by L1B_rad. An analogous scheme applies to the DC product image cubes.**

### 4.3.2 Gain flagging

The processing of each pixel depends crucially on whether it has been operated in low- or high-gain mode. It is thus convenient to derive a gain mask for the image cube of each camera.

In the case of the VNIR camera, which is operated with an automatic gain setting during the imaging phase of Earth datatakes, the 14th bit of the pixel value indicates its gain (0 for low gain, 1 for high gain). The VNIR (low-)gain mask is then derived as follows:

$$m_{\mathrm{LG}}(i,j,k) = [X(i,j,k) < 2^{13}] \quad \text{(VNIR)}\,. \tag{4.3-1}$$

The SWIR camera is instead operated with a fixed gain setting during the imaging frames of Earth datatakes, where a pre-defined (but configurable) set of channels is in low-gain mode and the remaining in high-gain mode:

$$m_{\mathrm{LG}}(i,j,k) = M_{LG}(j) \quad \text{(SWIR)}\,, \tag{4.3-2}$$

where $M_{LG}$ is the SWIR channel low-gain mask taken from CTB_RAD (cf. [AR-11]). Note that the SWIR gain mask has also been extracted from the virtual channel during L0 processing and saved to L0 metadata, but that mask is not reliable due to hardware limitations, cf. [AR-19]. Typically, SWIR channels are in low-gain mode up until a given wavelength and in high-gain mode thereafter. During the dark phases, the SWIR gain is as for VNIR, namely 128 low-gain frames for all channels followed by 128 high-gain frames.

The gain masks above are derived separately for the imaging and dark phases of each camera.

### 4.3.3 Raw quality

In this step the uncalibrated “raw” Detector Maps are generated; please refer to Sec. 4.4 for a full description.

### 4.3.4 Non-linearity correction

The first step in the calibration of the instrument is to correct for the non-linear response function of the pixels, especially important close to the borders of the sensitivity range. During the design of the non-linearity correction algorithm by OHB, two important effects were identified that need to be mitigated before the actual non-linearity correction, namely the VNIR line offset and the SWIR electronic offset. For a detailed discussion on these effects, please refer to [AR-4].

#### 4.3.4.1 VNIR line offset

It has been observed that the VNIR camera, when illuminated, presents an offset for pixels operated in high-gain mode. The offset is scene-dependent and it varies with spectral channel, but it is roughly homogeneous in the spatial direction. Therefore, the non-illuminated spatial pixels at the extremes of the detector (cf. Figure 4-3) can be used to estimate the offset. Typically, 4 pixels in each side are used; the exact number and location of the side pixels are stored in the pixel mask in CTB_LIN (cf. [AR-11]).

The first step is to compute the average dark signal for the side pixels of each spectral channel:

$$L_d(j) = \frac{1}{N_F N_s} \sum_{i=1}^{N_F} \sum_{k \in K_s} X_{\mathrm{pre/post\,HG}}(i,j,k)\,. \tag{4.3-3}$$

where the high-gain pre and post dark frames are concatenated in $X_{\mathrm{pre/post\,HG}}$, $N_F$ is the number of corresponding frames (typically, 256), $K_s$ is the set of side pixels as defined in the pixel mask in CTB_LIN and $N_s$ their number (typically, 8). Next, the average imaging signal for the side pixels of each spectral channel is computed for each frame:

$$L_i(i,j) = \frac{1}{N_s} \sum_{k \in K_s} X(i,j,k) \ . \tag{4.3-4}$$

where $X$ represents the imaging (L0) signal. Finally, the line offset is estimated as

$$\Delta L(i,j) = L_i(i,j) - L_d(j) \ . \tag{4.3-5}$$

and the correction reads

$$X_{HG}(i,j,k) = X_{HG}(i,j,k) - \Delta L(i,j) \ . \tag{4.3-6}$$

Note that the above correction is applied solely to VNIR high-gain pixels and is intended for imaging frames only.

#### 4.3.4.2 SWIR electronic offset

The electronic offset present in the SWIR camera needs to be corrected for both imaging and dark frames:

$$X(i,j,k) = X(i,j,k) - T_{\mathrm{EO}}(j,k) \ , \tag{4.3-7}$$

where $T_{\mathrm{EO}}$ represents the electronic offset calibration tables in CTB_LIN (cf. [AR-11]), one for each gain. Note that the above correction applies to SWIR only.

Due to the read-out process, the electronic offset of the first read-out SWIR spectral channel cannot be correctly estimated and therefore this spectral channel is flagged during L1B_rad for later processing by quality control. The first read-out SWIR channel is identified with the help of the SWIR integration time configuration stored in the virtual channels. In particular, for datatakes using the SWIR nominal integration time as in the case of Earth datatakes, the affected channel is the largest wavelength one, which is anyway non-illuminated and discarded during trimming (cf. Sec. 4.3.1).

#### 4.3.4.3 Non-linearity look-up tables

After the L0 data has been corrected for VNIR line offset and SWIR electronic offset, the actual non-linearity correction is done for each pixel individually through non-linearity look-up tables $T_{\mathrm{NL}}$ (cf. CTB_LIN in [AR-11]):

$$X(i,j,k) = T_{\mathrm{NL}}(j,k,X(i,j,k)) \ . \tag{4.3-8}$$

The correction is applied to both dark and imaging phases and with a different look-up table for each camera and each gain. Figure 4-4 illustrates schematically the effect of the non-linearity correction for an individual pixel.

Recall that the L1B_rad input images (i.e., L0 and DC spectral images) are unsigned 16-bit integers. After this correction, the spectral image contains 32-bit float values and is kept so throughout the L1B_rad processor for convenience.

A comment is in order here regarding the use of the calibration tables in L1B. All L1B-related calibration tables (i.e., CTB_{RAD,SPC,LIN,_DS,DPM}) are stored for the maximum configuration used in calibration datatakes, cf. [AR-11]. It is thus necessary to subset the calibration tables before their use in Equation (4.3-8) and other in the coming sub-sections. The different spectral and spatial dimensions of calibration tables, L0 products and L1B images is sketched in Figure 4-5. The subsetting in the spatial direction is straightforward, but it is non-trivial in the spectral direction, especially for SWIR. This operation is done with the help the list of non-illuminated pixels and of standard bands present in the calibration table metadata. For the non-linearity calibration tables CTB_LIN, because the tables are of considerable size (cf. [AR-11]), special care is taken to keep the used memory under control.

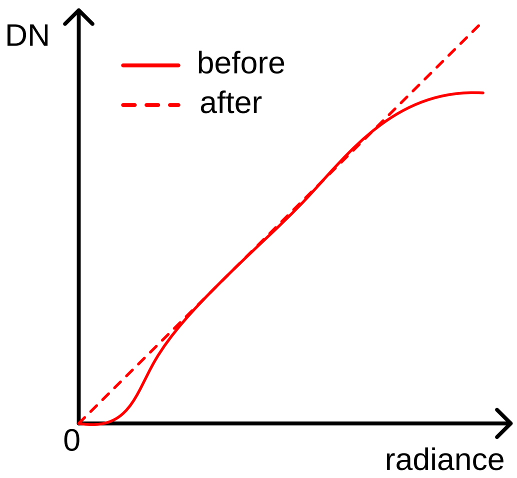


**Figure 4-4** **Non-linearity correction of an individual pixel. The plot shows the pixel values in digital numbers before and after non-linearity correction as a function of the incident radiance. Note that this plot is only illustrative and not to take at face value.**

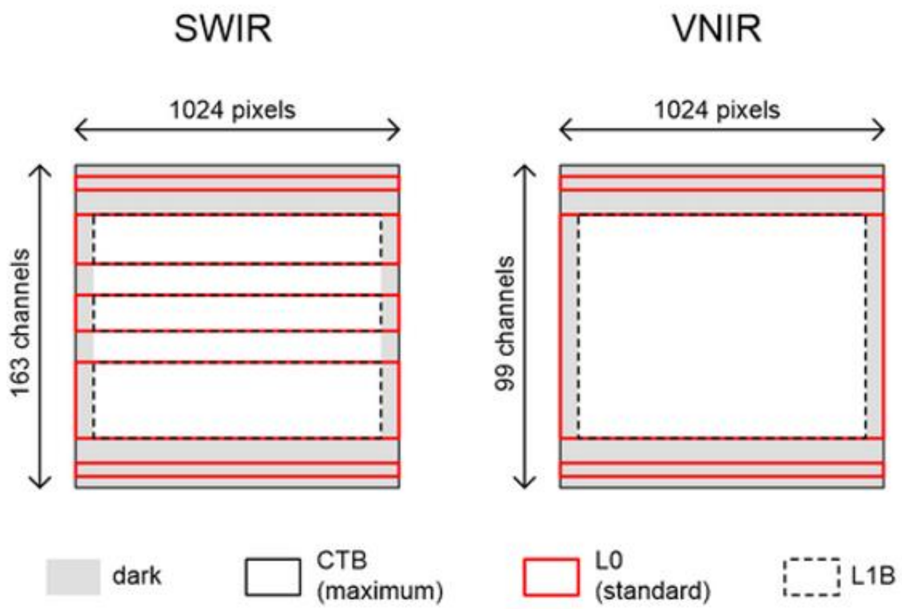


**Figure 4-5** **Subsetting of a calibration table for use in L1B_rad.**

#### 4.3.5 Dark signal and digital offset correction

The dark signal of the cameras is computed with the help of the dark measurements before and after the imaging phase stored in the DC product ($X_{\text{pre}}$ and $X_{\text{post}}$, respectively), which have already been corrected for non-linearity in the previous step, cf. Sec. 4.3.4. The computation involves the steps outlined in the following.

1. Subtract the digital offset $D_0$ (a constant for each camera):

$$X_{\text{pre,post}}(i,j,k) = X_{\text{pre,post}}(i,j,k) - D_0\ . \qquad (4.3\text{-}9)$$

2. For SWIR, correct the dark signal for the residual shutter thermal emission:

$$X_{\text{pre,post}}(i,j,k) = X_{\text{pre,post}}(i,j,k) - T_{\text{DS}}(j,k)\ , \qquad (4.3\text{-}10)$$

   where $T_{\text{DS}}$ represents the deep space calibration tables (cf. CTB__DS in in [AR-11]), one for each gain. This correction is not performed for the VNIR camera, because the expected thermal emission of the shutter at VNIR wavelengths is negligible.

3. Filter outliers for each dark image cube. This is done in two steps. First, the bottom and top $p$-percentiles are removed:

$$X_{\text{pre,post}}(i,j,k) = X_{\text{pre,post}}(i,j,k)[b_{j,k}^{p} \leq\ X_{\text{pre,post}}(i,j,k) \leq t_{j,k}^{p}]\ , \qquad (4.3\text{-}11)$$

   where $b_{j,k}^{p}$ and $t_{j,k}^{p}$ are the bottom and top $p$-percentiles of the frame distribution of channel/pixel $(j,k)$, respectively. The percentile $p$ is configurable and its default value is 0.03. Second, the $n$-sigma outliers of the remaining distribution are also removed:

$$X_{\text{pre,post}}(i,j,k) = X_{\text{pre,post}}(i,j,k)[\mu_{j,k} - n\sigma_{j,k} \leq\ X_{\text{pre,post}}(i,j,k) \leq \mu_{j,k} + n\sigma_{j,k}]\ , \qquad (4.3\text{-}12)$$

   where $\mu_{j,k}$ and $\sigma_{j,k}$ are the mean and standard deviation of the frame distribution of channel/pixel $(j,k)$, respectively. The parameter $n$ is configurable and its default value is 2.5. Finally, the frame-average of the filtered cubes is computed and stored in $\bar{X}_{\text{pre,post}}(j,k)$.

   Note that the filtering is done separately for each detector element (channel/pixel) and separately for each gain and each dark phase. Note as well that if one of the dark phases is completely missing (due to transmission losses) or filtered out, then only the other phase is used for computing the mean dark signal.

4. Compute the dark signal cube matching the imaging phase cube either by simple average of the pre and post dark phases or by time interpolation:

   simple average: $$X_{\text{d}}(i,j,k) = \frac{1}{2}\left(\bar{X}_{\text{pre}}(j,k) + \bar{X}_{\text{post}}(j,k)\right)\ , \qquad (4.3\text{-}13)$$

   time interpolation: $$X_{\text{d}}(i,j,k) = \bar{X}_{\text{pre}}(j,k) + \frac{t_i - t_{\text{pre}}}{t_{\text{post}} - t_{\text{pre}}}\left(\bar{X}_{\text{post}}(j,k) - \bar{X}_{\text{pre}}(j,k)\right)\ , \qquad (4.3\text{-}14)$$

   where $t_i$ is the time stamp of frame $i$ in the imaging phase, while $t_{\text{pre,post}}$ are the average times of the pre and post dark phases. Note that for VNIR these times are not corrected for jitter, which induces a very small error anyway since the VNIR jitter correction is in general much smaller than the sampling time.

The dark signal and digital offset correction follows then as

$$X(i,j,k) = (X(i,j,k) - D_0) - X_{\mathrm{d}}(i,j,k)\ . \qquad (4.3\text{-}15)$$

The correction is applied for each camera and each gain separately. Note that the digital offset is applied after non-linearity and equally to the imaging and dark phases, so it actually cancels out in Equation (4.3-15). However, for consistency with [AR-4], the digital offset correction is kept here.

It is also important to point out that for particularly dark regions in the imaging phase (e.g., water at SWIR wavelengths), the corrected image value from Equation (4.3-15) can be negative. At this stage, negative values are zeroed-out and they are flagged by the quality routines (cf. Sec. 4.4) and appropriately interpolated in L1B_int (cf. [AR-15, AR-23]).

### 4.3.6 Gain matching

Figure 4-6 shows the response function of a pixel in high or low-gain mode after the non-linearity and dark signal corrections. Clearly, given the gain mode of a pixel and the slope of the corresponding curve in Figure 4-6, it is possible to estimate the incident radiance, i.e. to radiometrically calibrate the pixel values.

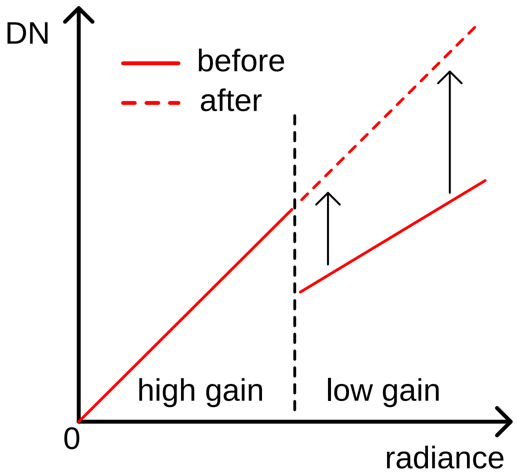


**Figure 4-6 Gain matching of low-gain pixels. The plot shows the pixel values in digital numbers before and after gain matching as a function of the incident radiance. Note that this plot is only illustrative and not to take at face value.**

However, the straylight correction (cf. Sec. 4.3.8) complicates this simple framework, because the signal from any given pixel has contributions from neighbouring (spatial and spectral) pixels, which can have a different gain. It is therefore necessary to match the trend of the high- and low-gain pixels before performing straylight correction. This is accomplished applying a gain matching coefficient to low-gain pixels:

$$\text{if } m_{\mathrm{LG}}(i,j,k) = 1\text{:}\ \ X(i,j,k) = X(i,j,k)T_G(j,k)\ , \qquad (4.3\text{-}16)$$

where $T_G$ is the gain coefficient table (cf. CTB_RAD in [AR-11]). A different table is available for SWIR and VNIR. Recall from Sec. 4.3.2 that an individual VNIR pixel can be in either low- or high-gain mode depending on the incident radiance (auto gain setting), while each SWIR pixel has always the same gain mode (fixed gain setting) for Earth datatakes. After gain matching the trend of low-gain pixels resembles the dashed line in Figure 4-6.

### 4.3.7 Response non-uniformity correction

Once gain matched, the data cube is corrected for response non-uniformity (RNU):

$$X(i,j,k) = X(i,j,k)T_{\mathrm{RNU}}(j,k) \; , \qquad (4.3\text{-}17)$$

where $T_{\mathrm{RNU}}$ is the RNU table (cf. CTB_RAD in [AR-11]). Similarly to gain matching, there is a set of tables for each camera.

The RNU tables mentioned above refer to the latest calibration measurement. For periods when there is significant VNIR sensor degradation between consecutive calibrations, coefficients for the time interpolation of VNIR RNU behaviour have been computed and saved in the radiometric calibration product CTB_RAD (cf. [AR-11], FQR RID WER-RO-0003, SCR-00322). When this is the case, the VNIR RNU coefficients for the particular datatake under consideration are given by

$$T_{\mathrm{RNU}}(j,k) = A(j,k)e^{B(j,k)t} + C(j,k)t^3 + D(j,k)t^2 + E(j,k)t + F(j,k) \; , \qquad (4.3\text{-}18)$$

where $A$ through $F$ are the coefficients in CTB_RAD and $t$ is the time of the datatake in number of days since April 1st, 2022.

### 4.3.8 Straylight correction

In any non-ideal detector, the signal of a given pixel is not only dependent on the light directed at that pixel but also on the light falling in neighbouring (spatial and spectral) pixels. The effect of this so-called straylight has to be undone in order to estimate the actual incoming radiance in each pixel. The magnitude and properties of straylight in EnMAP have been studied in [AR-25, AR-26] (see also [AR-4]), including diffuse straylight, ghosts, along-track out-of-field straylight and across-track out-of-field straylight. A diffuse straylight correction algorithm has been proposed in [AR-26]. A short description of the proposed algorithm is given here along with the adaptations needed for L1B processing. Note that the correction algorithm only corrects for diffuse straylight; for a discussion on out-of-field straylight and ghosts, please refer to [AR-26].

#### 4.3.8.1 Straylight extraction matrix

The straylight extraction matrix encodes the normalised amount of diffuse straylight across the whole detector for any given illuminated pixel. This is the key element of the straylight correction algorithm and it has been provided following the characterisation and calibration campaign [AR-24, AR-26]. Unlike other calibration tables, the straylight extraction matrix is not supposed to be updated during the whole mission lifetime and is thus part of the S-310 processor. Its format is described in Table 4-1 and in the following.

| **Straylight extraction matrix product** | | | |
|---|---|---|---|
| **File name** | **Description** | **Format** | **Size** |
| ENMAP01-CTB_SLC-20220401T000000Z_V000002_20211112T170000Z-STRAYLIGHT_SWIR.BIN | Straylight extraction matrix for SWIR | binary (4-byte float) | 1.2 Gbyte |
| ENMAP01-CTB_SLC-20220401T000000Z_V000002_20211112T170000Z-STRAYLIGHT_VNIR.BIN | Straylight extraction matrix for VNIR | binary (4-byte float) | 0.4 Gbyte |

**Table 4-1 Description of straylight extraction matrix product in S-310 processor.**

The straylight properties of both SWIR and VNIR were derived in the illuminated area only (156x1000 for SWIR-A, 91x1000 for VNIR) and in bins of 3 spectral pixels by 3 spatial pixels. The straylight extraction matrix consists thus of a 4D tensor with dimensions 52x334x52x334 for SWIR-A and 31x334x31x334 for

VNIR and is placed as received from the Space Segment (see [AR-24]) under DATA/CTB_SLC in the S-310 processor. The matrix has been saved with the spatial direction first, in double precision and in Fortran style (column-major). Note that widely used programming languages such as C and Python use native row-major ordering. In addition, for SWIR the spectral direction is inverted as in SWIR raw data, i.e. the wavelength decreases for increasing spectral channel index. This channel inversion in SWIR has to be undone for use in L1B processing. For clarity, the following pseudo-code in Python using NumPy illustrates how the SWIR straylight extraction matrix may be loaded:

```
import numpy as np

# Load binary file
npix, nch = 334, 52
f = ‘DATA/CTB_SLC/ENMAP01-CTB_SLC-20220401T000000Z_V000002_’ +\
    ‘20211112T170000Z-STRAYLIGHT_SWIR.BIN’
sl_mat = np.memmap(f, dtype='float32', mode='r',shape=(npix*nch, npix*nch))

# Swap Fortran style (column-major) to C style (row-major)
sl_mat = sl_mat.transpose()

# Reshape as 4D tensor
sl_mat = sl_mat.reshape(npix, nch, npix, nch)

# Swap to channels first
sl_mat = np.swapaxes(sl_mat, 0, 1)
sl_mat = np.swapaxes(sl_mat, 2, 3)

# Invert ordering of channels (for SWIR only)
sl_mat = sl_mat [::-1,:,::-1,:]
```

The loading of the VNIR straylight extraction matrix is analogous to the example above (with npix, nch = 334, 31), but there is no need to invert the channel ordering.

Note that the straylight extraction matrix has been derived for the illuminated areas of the instruments during the calibration campaign. Small shifts of the illuminated areas are to be expected during and after launch, so the available straylight extraction matrix is strictly speaking not applicable to the illuminated area during operations. This has a negligible impact on the correction, because straylight presents a very slow dependence along the spectral and spatial directions so that small shifts of a few pixels do not greatly affect the amount of estimated straylight.

Note as well that straylight has only been characterised for SWIR-A and VNIR. In case the redundant SWIR-B ever needs to be put into use, either the SWIR-A straylight extraction matrix shall be applied assuming similar straylight properties in both detectors, or the straylight correction shall be turned off altogether.

#### 4.3.8.2 Straylight correction algorithm

The principle of the diffuse straylight correction algorithm proposed in [AR-26] is conceptually straightforward: apply the straylight extraction matrix to the (RNU-corrected) image frame to estimate straylight and then subtract the latter from the frame. The whole algorithm is applied independently for each image frame. Despite the conceptual simplicity, there are several details that need to be taken into account before this algorithm can be implemented in L1B processing.

Firstly, since straylight mixes neighbouring pixels, it is important to treat dead pixels appropriately so that they do not spoil the correction in the neighbouring pixels. Therefore, for the purposes of straylight correction only, dead pixels are filled in with the mean of their neighbouring (valid) pixels in the straylight bins of 3 spectral pixels by 3 spatial pixels. This masked mean $\bar{X}_{3\text{x}3}$ maybe derived from the initial image cube $X$ as follows:

$$\bar{X}_{3\text{x}3} = D_{3\text{x}3}(X; m_{\text{DPM}}) \; , \tag{4.3-19}$$

where $D_{3\text{x}3}(A; M)$ represents the downsampling operation by averaging $A$ over 3x3 bins ignoring pixels in mask $M$, and $m_{\text{DPM}}$ is the 2D mask identifying all dead pixels (cf. CTB_DPM in [AR-11]). The mean $\bar{X}_{3\text{x}3}$ can then be upsampled to the original image dimensions:

$$\bar{X} = U_{3\text{x}3}(\bar{X}_{3\text{x}3}) \; , \tag{4.3-20}$$

where $U_{3\text{x}3}(A)$ denotes the upsampling operation of $A$ by repetition over 3x3 bins. With the above definitions, the filling in operation may be written for each image frame as

$$X'(i, m_{\text{DPM}}) = \bar{X}(i, j, k) \; . \tag{4.3-21}$$

Secondly, the image data accessible during L1B processing does not exactly correspond to the straylight scene for which the straylight extraction matrix was obtained. This is illustrated in Table 4-2. Before the straylight extraction matrix can be applied, the image data has then to be fitted to the straylight scene. The non-illuminated channels and pixels have already been trimmed at the beginning of L1B processing (cf. Sec. 4.3.1). This is usually enough to bring the VNIR image cube to the straylight scene dimensions. For SWIR, however, channels in the water absorption bands are not transmitted for Earth datatakes and are thus missing from the SWIR L1B image cube (see Figure 4-5). These missing SWIR channels are filled in with zeros in the appropriate positions. This is done by defining a zero-valued image cube of the dimensions of the straylight scene and assigning the illuminated standard bands to $X'$:

$$X'' = 0 \quad , \quad X''(i, m_{\text{std}}, k) = X'(i, j, k) \; , \tag{4.3-22}$$

where $m_{\text{std}}$ is the 1D mask identifying the illuminated standard bands in the straylight scene.

| | SWIR-A | VNIR |
|---|---|---|
| physical dimensions | 256 x 1024 | 256 x 1056 |
| L0 scene (standard configuration) | 135 x 1024 | 95 x 1024 |
| L1B scene | 131 x 1000 | 91 x 1000 |
| straylight scene | 156 x 1000 | 91 x 1000 |
| straylight extraction matrix | $(52 \times 334)^2$ | $(31 \times 334)^2$ |

**Table 4-2 Different dimensions for SWIR-A and VNIR. All dimensions are in channels x pixels.**

The core of the straylight correction algorithm may now be applied. The image data is first downsampled to the straylight resolution by averaging over the straylight bins of 3 spectral pixels by 3 spatial pixels. Note that the dead pixels have already been filled in, so there is no need at this point to implement a masked average downsampling. Any padding needed to make the scene dimensions divisible by the 3x3 bins is done by appending zero-valued bands and/or pixels before performing the downsampling operation. For example, the SWIR scene of dimensions 156x1000 needs no padding in the spectral direction since 156 is divisible by 3, but needs 2 padded pixels so that the padded spatial dimension 1000+2 is divisible by 3. The downsampled image data is written as

$$X_{3\text{x}3} = D_{3\text{x}3}(X'') \; . \tag{4.3-23}$$

Next, the straylight estimate is obtained by multiplying the straylight extraction matrix $T_{\text{SL}}$ defined in Sec. 4.3.8.1 and the downsampled image $X_{3\text{x}3}$:

$$X_{\text{SL},3\text{x}3} = X_{3\text{x}3} T_{\text{SL}} \; . \tag{4.3-24}$$

The straylight estimate at full resolution is then obtained by upsampling by repetition and passing a Gaussian filter:

$$X_{\mathrm{SL}} = U_{3\mathrm{x}3}(X_{\mathrm{SL},3\mathrm{x}3}) \,, \tag{4.3-25}$$
$$X_{\mathrm{SL}} = \mathrm{G}(X_{\mathrm{SL}};\sigma) \,, \tag{4.3-26}$$

where $\mathrm{G}$ represents a 2D Gaussian filter over spatial and pixel directions with unit standard deviation $\sigma = 1$.

The upsampled straylight estimate $X_{\mathrm{SL}}$ has now to be fitted back to the original scene (cf. Table 4-2). In particular, any padding done before the downsampling operation in Equation (4.3-23) has to be undone. Moreover, for the case of SWIR, the water absorption bands added in Equation (4.3-22) have now to be removed. For the processing of calibration datatakes (in S-320, not relevant for L1B), the SWIR water absorption bands do not need to be removed. In addition, for those datatakes, a straylight estimate is needed also for the dark pixels and channels. This is achieved by padding the straylight-to-signal ratio found in the illuminated area at constant values, unless the signal is zero, in which case a zero straylight is assumed.

After these operations are performed on the straylight estimate $X_{\mathrm{SL}}$, the final step is to subtract it from the original image data:

$$X(i,j,k) = X(i,j,k) - X_{\mathrm{SL}}(i,j,k) \,. \tag{4.3-27}$$

### 4.3.9 Radiometric calibration

The last step of the calibration procedure consists of applying the radiometric coefficients to each pixel:

$$X(i,j,k) = X(i,j,k)T_{\mathrm{R}}(j) \,, \tag{4.3-28}$$

where $T_{\mathrm{R}}$ is the calibration coefficient table (cf. CTB_RAD in [AR-11]). There is a separate table for each camera. The radiometric coefficients are the high-gain ones since in gain matching all pixels have been matched to the high-gain trend, cf. Figure 4-6.

Analogously to RNU in Sec. 4.3.7, also the VNIR radiometric coefficients may vary significantly between calibration measurements for some periods of time. In such cases, the radiometric calibration product CTB_RAD includes appropriate coefficients for the interpolation of the VNIR radiometric calibration of each band (cf. [AR-11], FQR RID WER-RO-0003, SCR-00322):

$$T_{\mathrm{R}}(j) = A(j)e^{B(j)t} + C(j)t^3 + D(j)t^2 + E(j)t + F(j) \,, \tag{4.3-29}$$

where $A$ through $F$ are the coefficients in CTB_RAD and $t$ is the time of the datatake in number of days since April 1st, 2022.

Note that, in case no straylight correction were needed, it would be possible to merge gain matching and radiometric calibration into a single step with a single multiplicative coefficient $T_{\mathrm{G}}(j,k)T_{\mathrm{RNU}}(j,k)T_{\mathrm{R}}(j)$, cf. Equations (4.3-16), (4.3-17) and (4.3-28). Alternatively, as discussed in Sec. 4.3.6, it would be possible to calibrate the low- and high-gain pixels with dedicated radiometric coefficients for each gain without the need for gain matching.

The output of L1B_rad contains the radiometrically calibrated image for both cameras, saved in BIL format with 32-bit float values of unit mW/cm$^2$/sr/µm. This is then further processed by the L1B_int sub-processor, cf. [AR-15, AR-23].

#### 4.3.10 Calibrated quality

Please refer to Sec. 4.4 for a full description of the calibrated quality routines.

### 4.4 Quality routines

As depicted within Figure 4-2, the QC routines are included in different steps of the L1B_rad processor. Reg the QC procedures, these are applied in the following sequence:

- <trimming and gain flagging, see Ch. 4.3.1 and 4.3.2>
- Creation of raw Detector Map (DM)
- <calibration steps, see Ch. 4.3.4 – 4.3.8>
- Check of the dimensions of the inputs (image cubes, DeadPixelMasks)
- Creation of calibrated Detector Map (DM)
- Readout band flagging (SWIR only)
- Check if the DSHA flag is provided by L1B
  - Include DSHA channel information in QC
- Background flagging
- *Spectral smile analysis (disabled as outcome of Commissioning Phase)*
  - *Check for cross-track scene homogeneity*
  - *If given, check for indication of spectral smile*
- Defective pixel flagging
  - Dead pixel flagging
  - Saturation, high and low radiance pixel flagging
  - Analysis and flagging of striping / banding artefacts
- Creation of the internal Defective Pixel Mask used for interpolation (DPM_int)
- Creation of QC metadata
- Creation of QC products (DPM, raw + calibrated DMs, QualityTestFlags)

If not noted otherwise, the steps are carried out for both VNIR and SWIR.

#### 4.4.1 Generation of the raw Detector Map

| **Input data** | **Output data** | **Auxiliary data** | |
|---|---|---|---|
| | | Before Launch | After Launch |
| • L0 EnMAP Data | • VNIR detector map (raw)<br>• SWIR detector map (raw) | - | - |

To support the monitoring of dead pixels, first the band-wise column means are calculated using the HSI data in uncalibrated raw DN. This is done separately for the VNIR and SWIR data. In the standard case the resulting outputs are two matrices with size of 1000 spatial pixels x 91 spectral pixels in VNIR and 1000 spatial pixels x 131 in SWIR.

The column mean DNs for detector element j,k can be calculated as:

$$\overline{DN}_{j,k} = \frac{1}{Ni}\sum_{i=1}^{Ni} DN_{i,j,k} \ , \qquad (4.4\text{-}1)$$

Where
DN – the raw Digital Number of the observation,
Ni - the total number of frames.

The raw Detector Map (as a single tar.gz file) is a component of the L0 / L1B / L1C / L2A Output Product. A full description and examples are provided in [AD-21].

### 4.4.2 Generation of the calibrated Detector Map

| **Input data** | **Output data** | **Auxiliary data** Before Launch | After Launch |
|---|---|---|---|
| • L1B EnMAP data (float) | • VNIR detector map (calibrated) (float)<br>• SWIR detector map (calibrated) (float) | - | - |

To support the data quality control, the band-wise column means are calculated using the fully processed HSI data in at-sensor radiance units. As before, this is done separately for the VNIR and SWIR data. In the standard case the resulting outputs are two matrices having the size of 1000 spatial pixels x 91 spectral pixels in case of the VNIR and 1000 spatial pixels x 131 spectral pixels in case of the SWIR.

The column mean radiance values for detector element j,k as well as the related standard deviation can be calculated as:

$$\overline{L}_{j,k} = \frac{1}{Ni}\sum_{i=1}^{Ni} L_{i,j,k}$$
$$\sigma L_{j,k} = \sqrt{\frac{1}{Ni}\sum_{i=1}^{Ni}(L_{i,j,k} - \overline{L}_{j,k})^2} \qquad (4.4\text{-}2)$$

Where

$\overline{L}_{j,k}$ : mean radiance value for image column j in band k over all scan lines i

$\sigma L_{j,k}$ : standard deviation of radiance values for image column j in band k over all scan lines i

Ni: total number of scan lines of the image.

The calibrated Detector Map (as a single tar.gz file, containing only the mean radiance and not the standard deviation) is a component of the L0 / L1B / L1C / L2A Output Product. A full description and examples are provided in in [AD-21].

### 4.4.3 Check of the dimensions of the inputs (image cubes, DeadPixelMasks)

| **Input data** | **Output data** | **Auxiliary data** Before Launch | After Launch |
|---|---|---|---|
| • L1B EnMAP data (float)<br>• Dead Pixel Mask | - | - | - |

In this step it is verified that the number of cross-track pixels (Nj) and spectral bands (Nk) of the VNIR and SWIR image cubes match with the size of the Dead Pixel Mask (Nj,Nk). If not, an error is issued and processing is stopped.

### 4.4.4 Readout band flagging (SWIR only)

| **Input data** | **Output data** | **Auxiliary data** Before Launch | After Launch |
|---|---|---|---|
| • L1B EnMAP data (float) | • Update of 3D array containing abnormal and dead pixels (DPM) (binary)<br>• Update of 3D array containing abnormal and dead pixels which are to be interpolated during L1B (DPM_int) (binary) | • SWIR readout bands | • SWIR readout bands |

As mentioned in Ch. 4.3.4.2, during the SWIR electronic offset correction not all channels can be processed, and are consequently flagged in the DPM and DPM_int.

### 4.4.5 DSHA band flagging

| **Input data** | **Output data** | **Auxiliary data** Before Launch | After Launch |
|---|---|---|---|
| • List of DSHA affected bands (generated within L0 processor) | Depending on configuration, either:<br>• Update of 3D array containing abnormal pixels (DPM) (binary)<br>or<br>• Update of 3D array containing abnormal and dead pixels which are to be interpolated during L1B (DPM_int) (binary) | - | - |

As a result of the Commissioning Phase, DSHA bands are flagged as abnormal pixels and are not interpolated.
Note that if the need shall arise (due to changes in instrument behaviour in Operational Phase) to *interpolate* the DSHA band, then the configuration (thresholds.json, set “interpol_DHSA” = 1) can be adjusted so that DSHA bands are treated as missing bands (i.e., background) and are consequently interpolated.

### 4.4.6 Background flagging

In order to ensure that all invalid non-illuminated pixels are flagged, all pixels set to the background value within the L0 processing [AR-19] are flagged in the DPM and DPM_int.

| **Input data** | **Output data** | **Auxiliary data** Before Launch | After Launch |
|---|---|---|---|
| • L1B EnMAP data (float) | • Update of DPM (binary)<br>• Update of DPM_int (binary) | • Background value | • Background value |

### 4.4.7 Defective pixel flagging

| **Input data** | **Output data** | **Auxiliary data** Before Launch | After Launch |
|---|---|---|---|
| • L1B EnMAP Data<br>• Calibrated Detector Map | • Update of DPM (binary)<br>• Update of DPM_int (binary) | • Preliminary dead pixel mask (from Calibration Tables)<br>• Allowed dynamic range<br>• Striping thresholds | • Dead pixel mask<br>• Allowed dynamic range<br>• Striping thresholds |

The flagging of defective pixels is defined within [AR-4] as the detection and flagging of all dead and abnormal pixels (see Figure 4-7 and Table 4-3) and will be described in the following subsections. As proposed within [AR-4] and [AR-11], not all classes of dead pixels and of abnormal pixels need to be interpolated in L1B_int processor. Thus, in addition to the complete Defective Pixel Mask (DPM, being part of the L0 / L1B / L1C / L2A Output Product), also the internal version DPM_int is generated which contains only defects to be interpolated. The interpolation of these pixels will be performed subsequently in the L1B_int processor.

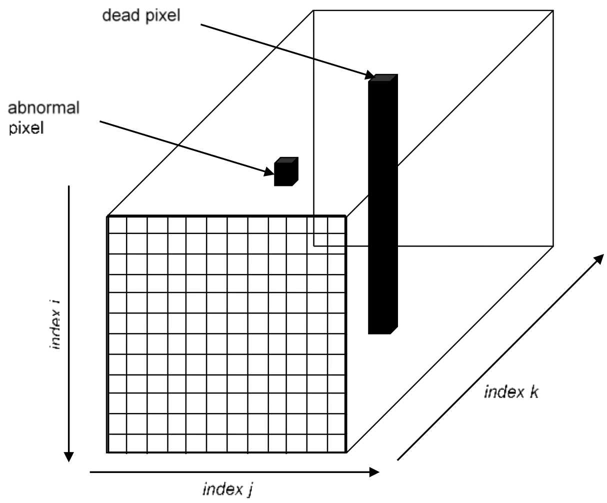


**Figure 4-7 Dead and abnormal pixel flagging.**

**Table 4-3 Bit coding of defective pixels; note that the final DPM and DPM_int are both binary.**

| Bit number | Pixel failure, if bit is set | Origin |
|---|---|---|
| 0 | dead (no recovery possible) | DeadPixelMask from S-320 |
| 1 | border pixel | DeadPixelMask from S-320 |
| 2 | hot | DeadPixelMask from S-320 |
| 3 | cold | DeadPixelMask from S-320 |
| 4 | flickering | DeadPixelMask from S-320 |
| 5 | stuck | DeadPixelMask from S-320 |
| 6 | readout low gain noise | DeadPixelMask from S-320 |
| 7 | readout high gain noise | DeadPixelMask from S-320 |
| 8 | linearity low gain defect | DeadPixelMask from S-320 |
| 9 | linearity high gain defect | DeadPixelMask from S-320 |
| 10 | PRNU defect | DeadPixelMask from S-320 |
| 11 | DSNU defect | DeadPixelMask from S-320 |
| 12 | low radiance defect | Abnormal pixel from L1B QC |
| 13 | high radiance defect and maximum radiance value | Abnormal pixel from L1B QC |
| 14 | striping/banding pixel | Abnormal pixel from L1B QC |
| 15 | readout/background pixel | - |

#### 4.4.7.1 Dead pixel flagging

The dead pixel mask [see AR-11] having the size of Ni, Nk is extended to a 3-D array, (Ni,Nj,Nk) with the defect flagged for all frames i (see Fig. 4-7). Note that the original Byte code of the Dead Pixel Mask is not changed (see Tab. 4-1), and converted to binary in the output step.

#### 4.4.7.2 Abnormal pixel flagging – saturation, blooming, high and low radiance

In this step all pixels (i,j,k) having a calibrated radiance value outside the allowed dynamic range are considered as abnormal pixels [AR-4] and are flagged.

**Table 4-4 Abnormal pixel flagging criteria**

| | | |
|---|---|---|
| Saturation | $L_{i,j,k}$ > $threshold_{saturation}$ | Band-specific, see description below. |
| High radiance | $L_{i,j,k}$ > $threshold_{high\_radiance}$ | $threshold_{high\_radiance}$ = 65535 |
| Low radiance | $L_{i,j,k}$ < $threshold_{low\_radiance}$ | VNIR $threshold_{low\_radiance}$ = 0.01<br>SWIR $threshold_{low\_radiance}$ = 0.0 |

For saturation, a bandwise threshold as proposed by OHB was confirmed during Commissioning Phase, which is based on the full well capacity (FWC) of the detectors thereby also taking the non-linearity at high radiance levels into account. The per-band threshold values and the observed radiances of saturated pixels are shown in Figure 4-8, confirming the thresholding.

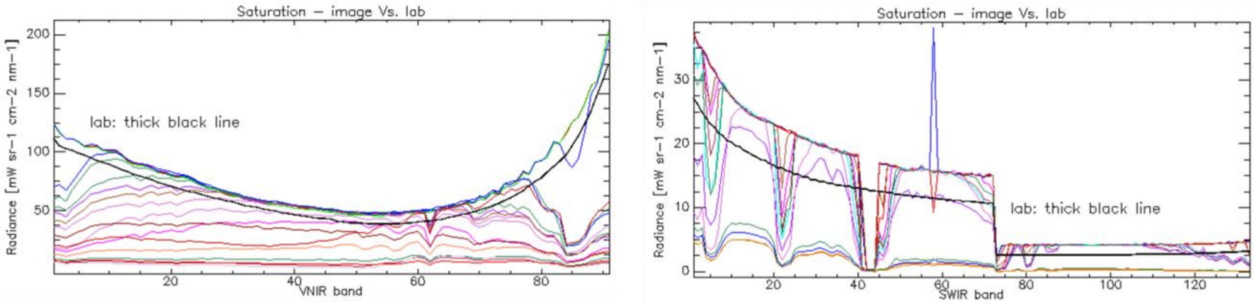


**Figure 4-8 Saturation thresholding. The thick black line corresponds to the per-band saturation values based on the FWC measured in the lab, and the thin colored lines are actual EnMAP image spectra of high-radiance targets.**

In order to correctly address the blooming in the SWIR, the saturation flag is also set for the same cross-track element and band in the subsequent frame, i.e. (i+1,j k) in case for SWIR saturation at (i,j,k).

Also note that in principle the usage of two thresholds on the upper radiance range is not necessary, but this allows for a separation between saturated pixels and pixels set to exceed the nominal range.

#### 4.4.7.3 Abnormal pixel flagging – striping / banding artefacts

Image defects like striping and banding can be detected using the calibrated Detector Map (see [AD-6] and [AD-21]). In order to do so, thresholds based on absolute difference in calibrated radiance units can be used:

$$
\begin{aligned}
&\left| \bar{L}_{j,k} - \bar{L}_{j+1,k} \right| > 1.6\ (VNIR)\ resp.\ 1.8\ (SWIR) && (spatial\ direction)\\
&\left| \bar{L}_{j,k} - \bar{L}_{j,k+1} \right| > 1.6\ (VNIR)\ resp.\ 1.8\ (SWIR) && (spectral\ direction)\\
&\left| \bar{L}_{j,k} - \bar{L}^{*}_{j,k} \right| > 1.6\ (VNIR)\ resp.\ 1.8\ (SWIR) && with\ \bar{L}^{*}_{j,k}\ being\ the\ lowpass-filtered\ version
\end{aligned}
$$

with $\bar{L}_{j,k}$ being the calibrated radiance value of the Detector Map corresponding to the cross-track element j and band k.

In the first two steps, the shift difference in spatial and in spectral dimensions of the calibrated DM are calculated. As a third analysis, also the absolute difference between the DM and a low-pass filtered DM is calculated, and all detector elements exceeding the threshold are flagged. This automated analysis is done for all bands without narrow atmospheric absorption features and having a nominal signal-to-noise performance, so consequently not all bands k are used. In order to provide a robust estimate, only detector elements included in the final flagging where all analysis steps agree (i.e., a detector element is detected using the shifting in spatial and spectral dimension, and the analysis using the filtered version). The flagging within the DPM and -if configured- in the DPM_int for a detector element j,k is then done for all frames I (see Fig. 4-7). During the Commissioning Phase the exclusion of the following band ranges was confirmed (assuming standard configuration): VNIR: bands 0-7, 69-72, 79-91; SWIR: bands 19-26, 37-49, 70-77 (related to the wavelength intervals of ~418 to ~449 nm, ~816 to ~839 nm, ~895 to ~993 nm; and ~1093 to ~1175 nm, ~1307 to ~1507 nm, ~1738 to ~1977 nm). If needed, these intervals can be adjusted in Operational Phase using the threshold refinement procedures

It is worth noting that an in-depth analysis for the cause of striping as well as the interfacing with the calibration in S-320 is carried out offline, as described within [AD-6] and [AD-21].

#### 4.4.7.4 Creation of the DPM and DPM_int

Within this processing step, the binary Defective pixel cubes (I,j,k) are created. Depending on the configuration, it can be set-up which defects are included in the Defective Pixel Mask used for the interpolation (DPM_int). The DPM being part of the Output Product always contains the full information, i.e. all defects are flagged.

In the current configuration, the pixel failures to be excluded in the DPM_int are 8, 9, 10, 11, 12, 13 (see Table 4-3). Thus, interpolated are all pixels flagged as “Dead”, “Border pixel”, “Hot” (White Defect), “Cold” (Black Defect), “Flickering”, “Stuck” and “Readout Noise Defect” in the DeadPixelMask, and pixels identified as “Striping Artefact” within the QC part of the L1B processor. Excluded form interpolation are “Linearity Defect”, “PRNU defect”, “DSNU defect”, “Saturated / High radiance defects” and “Low radiance defects”.

### 4.4.8 Analysis for spectral smile indications

As a result of the pre-flight laboratory characterizations and confirmed in the Commissioning Phase, the instrument performance regarding spectral smile and spectral stability are within requirements.
As described within [AD-6] and [AD-21], the analysis for spectral smile within an automated L0/L1B processor can’t be as accurate as an interactive process, especially when also modeling for the atmospheric conditions and the underlying Earth surface.
Consequently, the spectral smile indication check is currently disabled and the output is set to “-999” (i.e., “not produced”).

If required, the following part within the L0/L1B processing can be activated:
The approach is that spectral smile causes different cross-track radiance gradients within the range of narrow atmospheric absorption regions (e.g., $O_2$ absorption around 760 nm) when compared to cross-track radiance gradients in spectral regions without narrow features. Using the Detector Map to eliminate random noise, the cross-track radiance profiles at wavelengths outside of atmospheric absorption features are therefore used for a check of cross-track homogeneity of the scene. But this check can only give an indication for spectral smile in case that the observed Earth datatakes have a suitable cross-track scene statistic.

In pseudocode:

For wavelength region $k_1$ without absorption features:

- Calculate mean cross-track vector $a_j$ for n bands before selected wavelengths $k_1$
- Calculate mean cross-track vector $b_j$ for n bands after selected wavelengths $k_1$
- Calculate mean cross-track vector $c_j$ for n bands around selected wavelengths $k_1$
- Calculate ratio vector $d_j = 0.5 * (a_j + b_j) / c_j$

- Low-pass filtering and removal overall radiance level of vector $d_j^*$ = smooth($d_j$) – smooth(mean($d_j$))
- Count nd of cross-track elements with $d_j^*$ > threshold (0.05)
- If nd > (0.1 * Nj): SCENE_HOMOGENEITY NOT GIVEN

If the scene is too heterogeneous in cross-track direction, as indicated by nd > 0.1*Nj, then the metadata entry for “smile indication” is set to “-999” for “not produced”, and no further analysis is conducted.
If this scene homogeneity is given, then the calculation is also carried out for selected bands before, after and within a narrow atmospheric absorption.

In pseudocode:

For wavelength region having a narrow absorption feature at wavelength $k_2$:

- Calculate mean cross-track vector $e_j$ for n bands before absorption feature $k_2$
- Calculate mean cross-track vector $f_j$ for n bands after absorption feature $k_2$
- Calculate mean cross-track vector $g_j$ for n bands within absorption $k_2$
- Calculate ratio vector $h_j = 0.5 * (e_j + f_j) / g_j$
- Low-pass filtering and removal overall radiance level of vector $h_j$* = smooth($h_j$) – smooth(mean($h_j$))
- Count nh of cross-track elements with $h_j$* > threshold (0.05)
- If nh > (nd + safety_threshold (0.02)): INDICATION FOR SMILE else NO SMILE INDICATION

If the cross-track derivation within the atmospheric absorption region is larger than the cross-track derivation outside a narrow feature region, as indicated by nh > (nd + 0.02), then an indication for spectral smile is given and the metadata entry “smile indication” is set to “1”. In this criterion is not met, no smile indication is given and the metadata entry is set to “0”.

As mentioned before, the instrument performance regarding spectral smile and spectral stability estimated during Commissioning Phase are well within requirements, so that this test is currently disabled but can be enabled if required.

### 4.4.9 Generation of data quality metadata

In addition to the Quality Quicklook image, also metadata related to the data quality is generated (see Table 4-1 below).

**Table 4-5 Quality indicators automatically generated during L1B processing.**

| QC Entry | Parameter |
|---|---|
| overallQuality | Overall data quality |
| overallQualityVNIR | Overall data quality (VNIR camera) |
| overallQualitySWIR | Overall data quality (SWIR camera) |
| qualityRadiometryVNIR | Overall data quality related to radiometric properties (VNIR camera) |
| qualityRadiometrySWIR | Overall data quality related to radiometric properties (SWIR camera) |
| stripingBandingVNIR | Artifacts related to radiometric calibration (per mille, VNIR camera) |
| stripingBandingSWIR | Artifacts related to radiometric calibration (per mille, SWIR camera) |
| saturationCrosstalkVNIR | Saturation, cross-talk, blooming (per mille, VNIR camera) |
| saturationCrosstalkSWIR | Saturation, cross-talk, blooming (per mille, SWIR camera) |
| generalArtifactsVNIR | Other artifacts / abnormal pixel (per mille, VNIR camera) |

| | |
|---|---|
| generalArtifactsSWIR | Other artifacts / abnormal pixel (per mille, SWIR camera) |
| deadPixelsVNIR | Number of dead pixels (from Instrument Monitoring) (VNIR camera) |
| deadPixelsSWIR | Number of dead pixels (from Instrument Monitoring) (SWIR camera) |
| defectivePixelsVNIR | Number of defective pixels (per mille, VNIR camera) |
| defectivePixelsSWIR | Number of defective pixels (per mille, SWIR camera) |
| smileIndicationVNIR | Indication for spectral smile / spectral de-calibration (VNIR camera) |
| smileIndicationSWIR | Indication for spectral smile / spectral de-calibration (SWIR camera) |
| sensorLogVNIR | Warning messages related to sensor (VNIR camera) |
| sensorLogSWIR | Warning messages related to sensor (SWIR camera) |
| processorLogVNIR | Warning messages in processor log (VNIR camera) |
| processorLogSWIR | Warning messages in processor log (SWIR camera) |
| | |
| status | Overall status of the tile based on Monitoring and QC information |

The parameters stripingBanding, saturationCrosstalk, generalArtifacts, defectivePixels and smileIndication are derived by the procedures described within the previous chapters. The total number of affected pixels (resp. the per mille of all detector elements) for the VNIR and SWIR camera are then stored within these metadata QC Entries.

Also the additional parameters are included in the metadata:

Flagging of data sets with reduced accuracy indicated by messages in sensor log:

- Parsing of ENMAP.HSI.L0-METADATA which includes the instrument screening results

Flagging of data sets with reduced accuracy indicated by messages in processor log:

- Parsing of ENMAP.HSI.L0-LOG and ENMAP.HSI.L1B-LOG

A single aggregated “Overall Quality” is provided for the whole data cube (VNIR + SWIR), and two additionally aggregated ratings for the VNIR and the SWIR are also provided.

The “Overall Quality” per camera (VNIR, SWIR) is estimated by the following procedure:

- Set overall accuracy to “nominal”
- Number of striping flags > 5% of all pix.: overall accuracy set to “reduced” (if not already “low”)
- Number of striping flags > 10% of all pix : overall accuracy set to “low”
- Number of saturation flags > 10% of all pix: overall accuracy set to “reduced” (if not already “low”)
- Number of saturation flags > 20% of all pix: overall accuracy set to “low”
- Number of artefact flags > 5% of all pix : overall accuracy set to “reduced” (if not already “low”)
- Number of artefact flags > 10% of all pix: overall accuracy set to “low”
- Number of dead pixels > 5% of all pix : overall accuracy set to “reduced” (if not already “low”)
- Number of dead pixels > 10% of all pix : overall accuracy set to “low”
- In case of missing parameters, overall accuracy is set to “not produced” and a warning message is issued

The single aggregated “Overall Quality” for the whole data cube (VNIR + SWIR) also includes the results of the screening processor, and is based on the following:

- Set overall accuracy to “nominal”
- Set to “reduced” if overallQualityVNIR and/or overallQualityVNIR is “reduced” and/or screeningStaus is “reduced” and/or instrumentStatus is “reduced”

- Set to “low” if overallQualityVNIR and/or overallQualityVNIR is “low” and/or screeningStaus is “low” and/or instrumentStatus is “low”
- In case of missing parameters, overall accuracy is set to “not produced” and an error message is issued

Note that this overall data quality rating can be updated by the quality control procedures in L1C and L2A processors.

For setting the “Status” value, the following procedure is applied:

- Read “status” from metadata, being previously set by Instrument Monitoring (value of specific.status is used)
- If specific_status includes the prefix “DSHA_” (e.g. DSHA_NOMINAL):
    - Number of striping flags > 5% of all pix: status is set to “DSHA_REDUCED” (if not already “DSHA_LOW”
    - Number of striping flags > 10% of all pix: status is set to “DSHA_LOW”
    - Number of missing bands >2% of all bands: status is set to “DSHA_REDUCED” (if not already “DSHA_LOW”
    - Number of missing bands > 5% of all bands: status is set to “DSHA_LOW”
    - In case of missing parameters, status is set to “failed” and an error message is issued
- If specific_status does not include the prefix “DSHA_” (e.g., NOMINAL):
    - Number of striping flags > 5% of all pix: status is set to “REDUCED” (if not already “LOW”
    - Number of striping flags > 10% of all pix: status is set to “LOW”
    - Number of missing bands > 2% of all bands: status is set to “REDUCED” (if not already “LOW”
    - Number of missing bands > 5% of all bands: status is set to “LOW”
    - In case of missing parameters, status is set to “failed” and an error message is issued

#### 4.4.10 Generation of data quality test flags

For the Quality Test Flags, the information on the defective pixels (abnormal and dead) is aggregated within a Quality Quicklook layer, see [AR-8] for a full description of the L0 product and [AR-9] for the L1B, L1C and L2A products. For consistency with existing Quality Flags generated for the MODIS, Landsat 8 or Hyperion missions, the bits are read from right to left, starting with Bit 0.

For VNIR:

| BIT | 7 | 6 | 5 | 4 | 3 | 2 | 1 | 0 |
|---|---|---|---|---|---|---|---|---|
| DESCRIPTION VNIR | artefactVNIR | NOT USED | saturationVNIR | NOT USED | interpolatedPixel | NOT USED | Overall Quality | |

For SWIR:

| BIT | 7 | 6 | 5 | 4 | 3 | 2 | 1 | 0 |
|---|---|---|---|---|---|---|---|---|
| DESCRIPTION SWIR | NOT USED | artefactSWIR | NOT USED | saturation SWIR | interpolatedPixel | NOT USED | Overall Quality | |

The Quality Information is encoded as follows:

For the double bit (0-1):

00: Nominal quality
01: Reduced quality
10: Low Quality
11: Not produced

For bit (3):

0: This condition does not exist at all, or for less than 5 bands (VNIR) / 8 bands (SWIR)
1: This condition exists for 5 / 8 or more bands

For the bits (4, 5, 6, and 7):

0: This condition does not exist at all, or for less than 10 bands (VNIR) / 14 bands (SWIR)
1: This condition exists for 10 / 14 or more bands

In the above, "interpolated" is derived from the DPM_int, "saturation" only includes the saturated pixels, and "artefacts" includes the striping / banding artefacts as well as the low and high radiance pixels.

The per-pixel "Overall Quality" is estimated by the following procedure:

- Set overall accuracy to "nominal"
- If a pixel is either interpolated and/or saturated and/or has artefacts in 10 % of all bands: overall accuracy is set to "reduced (if not already "low") for this flag pixel
- If a pixel is either interpolated or saturated or has artefacts in 20 % of all bands: over accuracy is set to "low" for this flag pixel

## 4.5 Destriping

During the EnMAP Flight Qualification Review, it was decided to implement a destriping correction to EnMAP image data (FQR RID WER-RO-0004, SCR-00351). Destriping is applied at L1B level (top-of-atmosphere radiances) as the last processing step, after radiometric calibration (L1B_rad) and defective pixel interpolation (L1B_int).

### 4.5.1 Across-track destriping

Striping in the across-track direction is corrected with an image-based algorithm developed by M. Brell (GFZ) and provided to the Ground Segment (under license EUPL-1.2) for integration in the L1B processor. The algorithm, described briefly in the following, is applied bandwise to all VNIR and SWIR bands after execution of the L1B_int sub-processor.

Let $B$ be a generic band image (frames x pixels). The first step is to compute the across- and along-track gradients $B_x$ and $B_y$ as well as their slightly smoothed versions $\bar{B}_x$ and $\bar{B}_y$ derived using a uniform filter. A mask of heterogeneous regions can then be constructed by thresholding on the high-frequency along-track gradient:

$$M_h = \left(\left|B_y - \bar{B}_y\right| > T\right) \quad , \tag{4.5-1}$$

with $T$ a threshold value taken to be the maximum of the 5th percentiles of the along-track distribution of $\left|B_y - \bar{B}_y\right|$. Next, the cumulated median across-track gradients are computed excluding heterogeneous regions:

$$B_x^* = \mathrm{sum}_x \left[\mathrm{med}_y\left[\bar{B}_x[\sim M_h]\right]\right] \quad , \tag{4.5-2}$$

where $\mathrm{med}_y$ represents the median in the along-track direction and $\mathrm{sum}_x$ the cumulative sum over the across-track direction. The smoothed behavior of the cumulated across-track gradients is obtained by applying a 3rd order Savitzky–Golay filter $F_{\mathrm{SG}}$ to $B_x^*$. Finally, the resulting high-frequency across-track gradient $(B_x^* - F_{\mathrm{SG}}(B_x^*))$ is subtracted from the original band $B$ to obtain the destriped band $B_0$:

$$B_0 = B - (B_x^* - F_{\mathrm{SG}}(B_x^*)) \quad . \tag{4.5-3}$$

## 4.6 Output

The SWIR and VNIR image cubes are processed independently. Therefore, as output the Level 1B processor produces two separate at-sensor radiance hyperspectral cubes which are not registered. These data cubes are registered and combined into one data cube in the Level 1C processor. The contribution of each sub-processor to the several components of the L1B product is specified in Figure 4-1. For a detailed description of the L1B product, please refer to [AR-9].

The spectral region from 0.9 to 1 µm contains overlapping channels from the VNIR and SWIR spectrometers. All channels will be processed and delivered to the user, but any existing at-sensor radiance offsets between overlapping channels should be treated carefully and investigated in the future.

# 5. List of On-Going TBC / TBD

Table 5-1 lists the on-going issues TBC (to be confirmed) and TBD (to be decided).

| Number | Type | Topic | Status | Section | Due |
|---|---|---|---|---|---|
| | | | | | |

**Table 5-1 TBC/TBD list.**